BIOCHEMISTRY
including biophysical chemistry & molecular biology

Article

pubs.acs.org/biochemistry

# A Color-Determining Amino Acid Residue of Proteorhodopsin

Yuya Ozaki,[†] Takayoshi Kawashima,[†] Rei Abe-Yoshizumi,[†] and Hideki Kandori*[,†,‡]

[†]Department of Frontier Materials, Nagoya Institute of Technology, Showa-ku, Nagoya 466-8555, Japan
[‡]OptoBioTechnology Research Center, Nagoya Institute of Technology, Showa-ku, Nagoya 466-8555, Japan

Supporting Information

**ABSTRACT:** Proteorhodopsin (PR) is a light-driven proton pump found in marine bacteria. More than 1000 PRs are classified as blue-absorbing ($\lambda_{max}$ ~ 490 nm) and green-absorbing ($\lambda_{max}$ ~ 525 nm) PRs. The color determinant is known to be at position 105, where blue-absorbing and green-absorbing PRs possess Gln and Leu, respectively. This suggests hydrophobicity at position 105 plays a key role in color tuning. Here we successfully introduced 19 amino acid residues into position 105 of green-absorbing PR in the membrane environment and investigated the absorption properties. High-performance liquid chromatography analysis shows that the isomeric composition of the all-*trans* form is >70% for all mutants, indicating little influence of different isomers on color tuning. Absorption spectra of the wild-type and 19 mutant proteins were well-characterized by the pH-dependent equilibria of the protonated and deprotonated counterion (Asp97) of the Schiff base, whereas the $\lambda_{max}$ values of these two states and the p$K_a$ value differed significantly among mutants. Although Gln and Leu are hydrophilic and hydrophobic residues, respectively, the $\lambda_{max}$ values of the two states and the p$K_a$ value did not correlate with the hydropathy index of residues. In contrast, the $\lambda_{max}$ and p$K_a$ were correlated with the volume of residues, though Gln and Leu possess similar volumes. This observation concludes that the $\lambda_{max}$ and p$K_a$ of Asp97 are determined by local and specific interactions in the Schiff base moiety, in which the volume of the residue at position 105 is more influential than its hydrophobicity. We suggest that the hydrogen-bonding network in the Schiff base moiety plays a key role in the $\lambda_{max}$ and p$K_a$ of Asp97, and the hydrogen-bonding network is significantly perturbed by large amino acid residues but may be preserved by additional water molecule(s) for small amino acid residues at position 105.

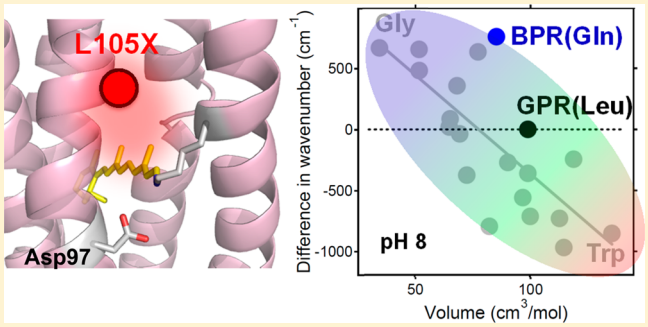


Microbial or animal rhodopsin contains either all-*trans* or 11-*cis* retinal, respectively, inside the seven transmembrane helices.[1] The retinal chromophore is bound to a lysine residue of the seventh helix via a protonated Schiff base linkage. The color tuning mechanism is an important topic in the field of rhodopsins because the color of a common molecule, either the all-*trans* or 11-*cis* retinal Schiff base, is determined by the surrounding amino acid residues of the protein.[2−8] While the mechanism is not fully understood, it is likely that color tuning is determined by various interactions between the retinal chromophore and protein, such as the electrostatic effect of charged groups, dipolar amino acid residues, aromatic amino acid residues, hydrogen bonding interactions, and steric contact effect.[1−8]

Proteorhodopsin (PR) is a light-driven proton pump found in marine γ-proteobacteria.[9,10] Because of the widespread distribution of proteobacteria in the world's oceanic waters, PR probably contributes significantly to global solar energy input in the biosphere. The absorption maxima of pigments are tuned to the depth at which specific bacteria live. Those living in the upper layers of the ocean absorb longer wavelengths, whereas those that exist in deeper layers absorb shorter wavelengths, consistent with the available light that penetrates the water.[11−13] Extensive genome analysis revealed the presence of thousands of PRs, which can be classified into blue-absorbing ($\lambda_{max}$ ~ 490 nm) PR (BPR) and green-absorbing ($\lambda_{max}$ ~ 525 nm) PR (GPR).[10] Previous studies showed that one of the determinants of color tuning of PR is at position 105, Gln in BPR and Leu in GPR.[13] The corresponding residue in a Haloarchaeal proton-pump bacteriorhodopsin (BR) is Leu93. X-ray crystallography showed that Gln and Leu are in direct contact with the 13-methyl group of the retinal chromophore in BPR[14] and *Exiguobacterium sibiricum* rhodopsin (ESR),[15] a homologous protein of GPR (Figure 1), respectively. Therefore, the L/Q (Leu/Gln) switch for color tuning is presumably caused by direct contact with the retinal chromophore.

Despite the publication of many structures of microbial rhodopsins, the molecular mechanisms of color tuning are poorly understood. The interhelical cavity of microbial rhopdopsins is divided by the Schiff base into extracellular and cytoplasmic "half-channels" that together describe the trajectory of transported protons.[1] The extracellular half-channel contains numerous charged or hydrogen-bonding residues as well as water molecules, whereas the cytoplasmic region is mostly hydro-

**Received:** July 9, 2014
**Revised:** September 1, 2014
**Published:** September 2, 2014

ACS Publications © 2014 American Chemical Society



dx.doi.org/10.1021/bi500842w | *Biochemistry* 2014, 53, 6032−6040

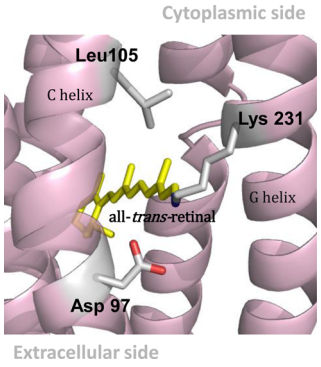


**Figure 1.** X-ray crystallographic structure of *E. sibiricum* rhodopsin (ESR) (Protein Data Bank entry 4HYJ) viewed from the B and C helix side. Shown as sticks are side chains of important amino acid residues, which are common between green-absorbing proteorhodopsin (GPR) and ESR. The number of residues is for GPR. The top and bottom regions correspond to the cytoplasmic (CP) and extracellular (EC) sides, respectively. The retinal chromophore bound to Lys231 is colored yellow. The nearest atom in the retinal chromophore from Leu105 is the 13-methyl carbon, and the distance between them is 4.1 Å.

phobic (Figure 1). The L/Q switch of PR is located in the cytoplasmic region, where the L-to-Q mutation in GPR[13] and the L-to-T mutation in BR[16] cause a spectral blue-shift. These facts suggest that introduction of polar groups at this position yields a spectral blue-shift and that nature selected L and Q at position 105 for GPR and BPR to detect green and blue light, respectively.

Here we performed a comprehensive mutation study of L105X GPR. We recently introduced a positively charged lysine group at this position of GPR, which was the first report of the introduction of a positive charge into the hydrophobic cytoplasmic domain of microbial rhodopsins.[17] In the study presented here, we replaced Leu105 with 19 amino acid residues, including K. Consequently, the 19 mutants at position 105 were successfully expressed, and their absorption properties were investigated. Unexpectedly, the $\lambda_{max}$ values of the two states, the protonated and deprotonated counterion (Asp97) of the Schiff base, and the p$K_a$ value did not correlate with the hydropathy index of residues. The $\lambda_{max}$ and p$K_a$ values did correlate with the volume of the residues, though Gln and Leu have similar volumes. The molecular mechanism of color tuning in PR is discussed on the basis of our results.

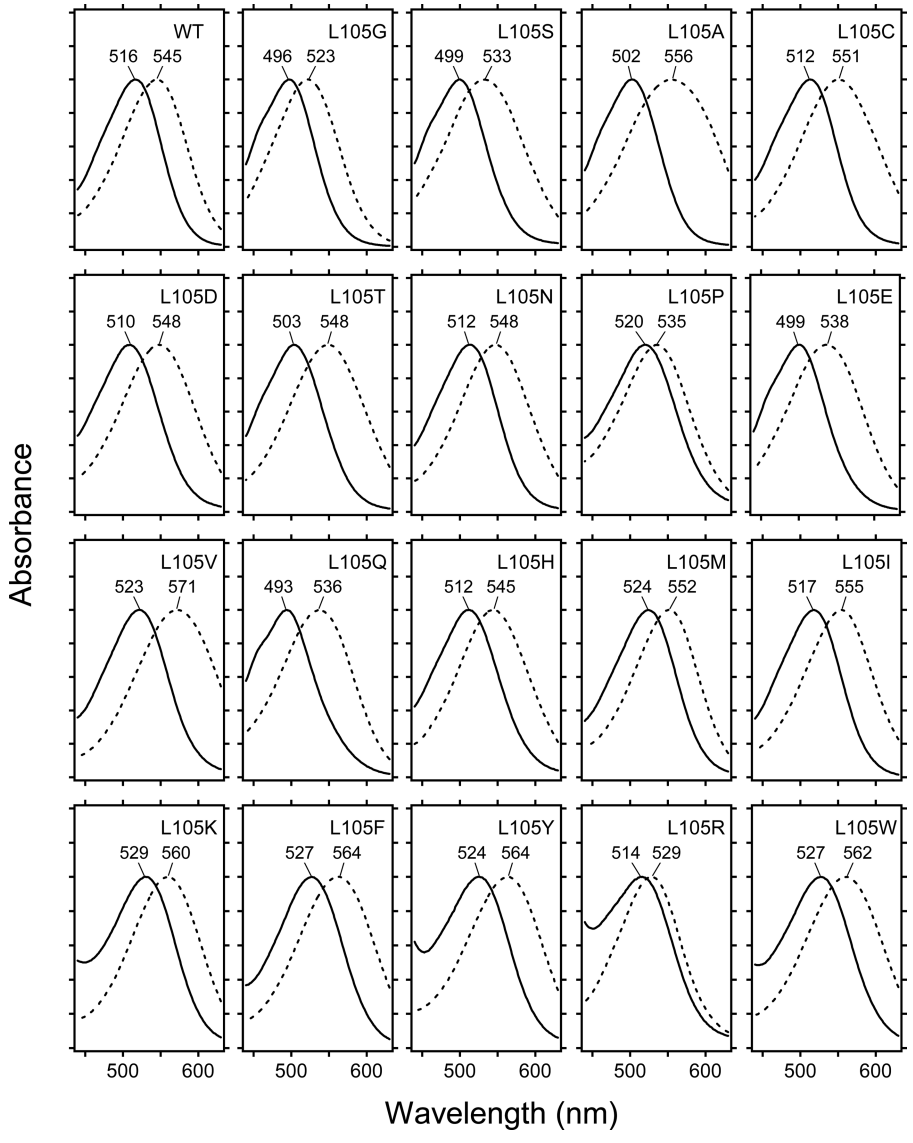


**Figure 2.** Absorption spectra of the wild type and 19 L105 mutants at low pH (---) and high pH (—). See Table 1 for actual pH values.


dx.doi.org/10.1021/bi500842w | *Biochemistry* 2014, 53, 6032−6040

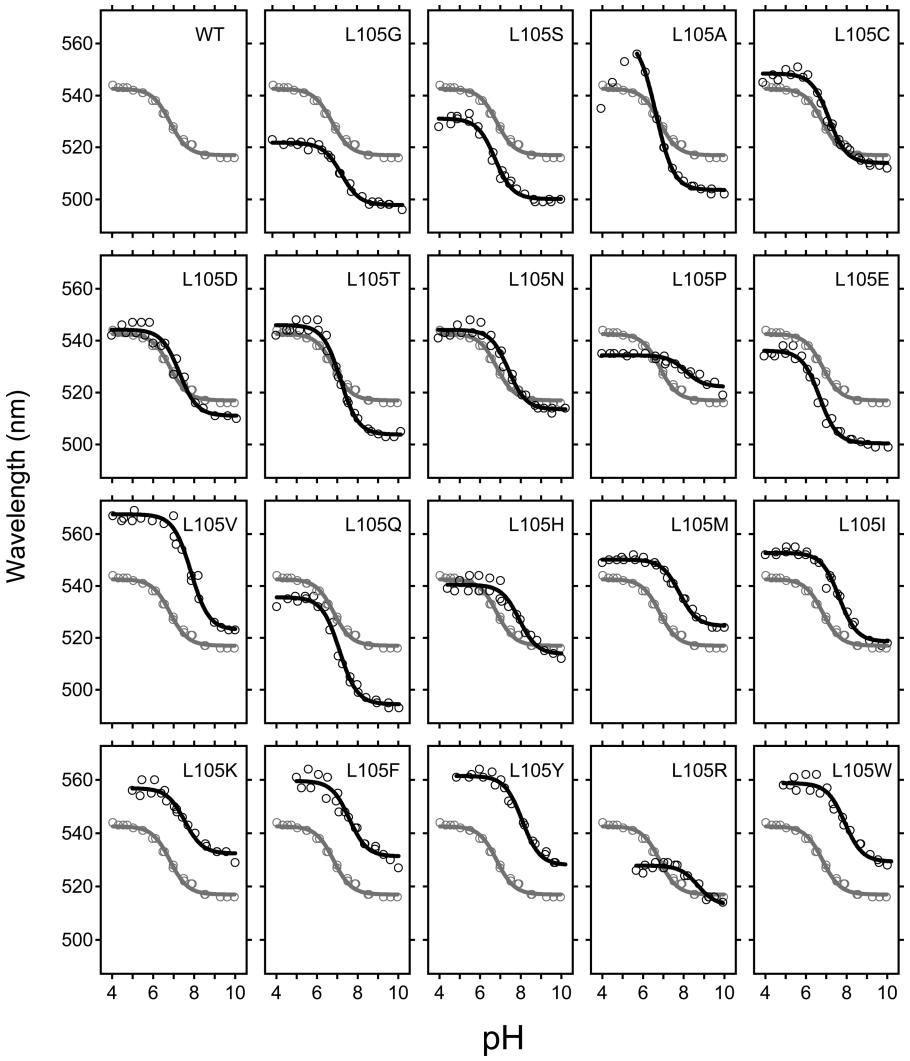


**Figure 3.** pH titration of the wild type (gray circles) and 19 L105 mutants (black circles). Lines represent the fits according to the Henderson–Hasselbalch equation.

## MATERIALS AND METHODS

**Expression and Purification of the L105X Mutant of GPR.** Expression plasmids were constructed as described previously.[17,18] To prevent oxidation of cysteine residues, a triple cysteine mutant (C107S, C156S, and C175S) was used as the template for mutagenesis.[18,19] We regarded this protein as the wild type and introduced additional mutations. Mutations were performed using the QuikChange site-directed mutagenesis kit (Stratagene) according to the manufacturer's protocol. Proteorhodopsin, having six histidines at the C-terminus, was expressed in *Escherichia coli*. The protein was solubilized with 0.1% *n*-dodecyl *β*-D-maltoside (DDM) and purified by Ni-NTA column chromatography.[17]

**UV–Visible Spectroscopy.** Absorption spectra of detergent-solubilized GPR (0.1% DDM, 150 mM NaCl, and 10 mM citric acid monohydrate, MES, MOPS, HEPES, CHES, and CAPS) were recorded using a Shimadzu UV-2400PC UV–visible spectrophotometer at 25 °C.[20,21] The initial pH was acidic, from which the pH was increased to 9–11 by the addition of NaOH. The absorption spectra were measured every 0.5 pH unit. Once the pH of the solution reached 9–11, it was again lowered to pH 4–6 by the addition of HCl. We confirmed that absorption spectra at the same pH produced by the addition of either NaOH or HCl were identical, indicating that pH titration was reversible between pH 4–6 and 9–11 for all proteins. The lowest and highest pH values for reversible titration are different for each protein, and such a pH was carefully selected for each protein (see Table 2). The absorption maxima were plotted as a function of pH, and the data were fit with the Henderson–Hasselbalch equation to determine the p$K_a$ of the counterion.

**High-Performance Liquid Chromatography (HPLC) Analysis.** HPLC analysis was performed as described previously.[22] A high-performance liquid chromatograph was equipped with a silica column (6.0 mm × 150 mm, YMC-Pack SIL). The solvent consisted of 12% (v/v) ethyl acetate and 0.12% (v/v) ethanol in hexane, and the flow rate was 1.0 mL/min. Extraction of retinal oxime from the sample was conducted with hexane after denaturation by methanol and 500 mM hydroxylamine at 4 °C. The molar composition of retinal isomers was calculated from the areas of the peaks in the HPLC patterns. Assignment of the peaks was performed by comparing them with the HPLC pattern from retinal oximes of authentic all-*trans* and 13-*cis* retinals. Three independent measurements were averaged.


dx.doi.org/10.1021/bi500842w | *Biochemistry* 2014, 53, 6032–6040

Table 1. Isomeric Composition of the Wild-Type and 19 Position 105 Mutant Proteins at Low and High pH

| | low pH (%) | | | | high pH (%) | | | |
|---|---|---|---|---|---|---|---|---|
| | all-*trans* | 13-*cis* | 11-*cis* | 9-*cis* | all-*trans* | 13-*cis* | 11-*cis* | 9-*cis* |
| wild type | 93.4 | 2.5 | 2.1 | 2.0 | 95.1 | 2.1 | 1.2 | 1.6 |
| L105G | 94.5 | 1.4 | 2.6 | 1.5 | 95.4 | 0.9 | 2.3 | 1.4 |
| L105S | 92.4 | 1.5 | 4.1 | 2.0 | 93.8 | 1.3 | 3.4 | 1.5 |
| L105A | 93.4 | 1.9 | 2.2 | 2.5 | 93.6 | 1.6 | 2.3 | 2.5 |
| L105C | 87.2 | 3.9 | 6.2 | 2.7 | 89.3 | 3.3 | 4.7 | 2.7 |
| L105D | 91.1 | 1.3 | 3.8 | 3.8 | 91.1 | 0.9 | 3.9 | 4.1 |
| L105T | 90.1 | 3.9 | 4.5 | 1.5 | 91.1 | 2.7 | 4.2 | 2.0 |
| L105N | 86.4 | 5.7 | 4.1 | 3.8 | 88.9 | 4.2 | 3.9 | 3.0 |
| L105P | 71.8 | 3.4 | 11.5 | 13.3 | 78.3 | 2.5 | 9.5 | 9.7 |
| L105E | 86.8 | 2.7 | 5.7 | 4.8 | 91.4 | 0.7 | 4.5 | 3.4 |
| L105V | 89.8 | 5.0 | 3.5 | 1.7 | 87.6 | 7.1 | 3.5 | 1.8 |
| L105Q | 82.9 | 3.7 | 7.2 | 6.2 | 88.1 | 2.4 | 6.0 | 3.5 |
| L105H | 89.3 | 5.1 | 3.2 | 2.4 | 90.4 | 4.1 | 3.4 | 2.1 |
| L105M | 91.0 | 2.4 | 3.3 | 3.3 | 94.2 | 1.8 | 2.2 | 1.8 |
| L105I | 86.0 | 4.1 | 2.4 | 7.5 | 90.3 | 2.7 | 1.5 | 5.5 |
| L105K | 90.9 | 2.4 | 2.4 | 4.3 | 92.0 | 2.6 | 2.2 | 3.2 |
| L105F | 84.9 | 4.6 | 4.3 | 6.2 | 84.0 | 6.4 | 4.7 | 4.9 |
| L105Y | 71.5 | 9.1 | 10.2 | 9.2 | 70.5 | 11.0 | 10.6 | 7.9 |
| L105R | 81.9 | 4.4 | 10.4 | 3.3 | 82.1 | 5.3 | 8.8 | 3.8 |
| L105W | 76.6 | 10.9 | 5.1 | 7.4 | 70.6 | 17.8 | 5.4 | 6.2 |

## RESULTS

**pH Titration of L105 Mutants.** The p$K_a$ of the Schiff base counterion in PR, Asp97, is located at a neutral pH,[23,24] indicating that both protonated and deprotonated forms exist at pH 7.0. It is thus important to examine the $\lambda_{max}$ of both protonated and deprotonated forms, as well as the p$K_a$ value by pH titration, which was performed on all L105 mutants and the wild type. The initial pH was acidic, and we first added NaOH stepwise and measured absorption spectra. After the sample pH reached a high value (9−11), HCl was added to lower the pH to 4−6. We confirmed that the absorption spectra at the same pH were identical between experiments with increasing and decreasing pH values, although the lowest and highest pH values differed for each protein.

Figure 2 shows absorption spectra of the wild type and 19 L105 mutants at low pH (dotted lines) and high pH (solid lines). Because the absorption spectra of most of the proteins at various pH values approximately exhibit a single isosbestic point (Figure S1 of the Supporting Information), only two forms, with protonated and deprotonated Asp97, are in equilibrium. It should be noted that in some mutants such as L105P, L105D, L105K, and L105R, the increase in pH caused deprotonation of the Schiff base to some extent ($\lambda_{max}$ < 400 nm), which complicates the analysis. However, even in that case, we are able to obtain accurate spectral information by monitoring $\lambda_{max}$ in the visible region (as shown in Figure 3). The $\lambda_{max}$ values of the wild type at low pH (protonated Asp97) and high pH (deprotonated Asp97) are 545 and 516 nm, respectively, which reproduced previous results.[21] Figure 3 shows pH titration curves of the wild type and 19 L105 mutants. In the case of the wild type, a fitting curve derived from the Henderson−Hasselbalch equation with $n$ = 1 indicated the p$K_a$ value to be 6.87.

Figure 3 demonstrates that absorption maxima of both protonated and deprotonated forms of Asp97 and p$K_a$ values are highly dependent on the amino acid residue at position 105. pH titration curves of L105C, L105D, and L105N are similar to that of the wild type but greatly deviate from those of the other mutants. This is an unexpected observation, because amino acid residues L, C, D, and N have no common properties. L105G and L105S clearly exhibit a spectral blue-shift, together with L105Q and L105E. In the case of L105Q, the residue of the L/Q switch, the blue-shift at high pH (495 nm) is larger than that at low pH (535 nm), and the blue-shift at pH 8, the physiological condition, is 499 nm. While small residues such as Gly and Ser cause a spectral blue-shift, large residues are likely to yield a spectral red-shift, as seen for L105V, L105M, L105K, L105F, L105Y, and L105W. In the case of L105I, the $\lambda_{max}$ is identical to that of the wild type at high pH, whereas a spectral red-shift was observed at low pH. In contrast, the $\lambda_{max}$ of L105T is similar to that of the wild type at low pH, whereas a spectral blue-shift was observed at high pH. This property of L105A is unique: $\lambda_{max}$ was more red- and blue-shifted than that of the wild type at low and high pH, respectively; consequently, $\lambda_{max}$ differs significantly (52 nm) between low and high pH. In addition, the $\lambda_{max}$ of L105A was blue-shifted at pH <5.5, suggesting the presence of another titratable group at pH <5.5. Similar spectral shifts were reported for BR[25] and SRII,[26,27] which originate from the binding of chloride to species with a protonated counterion. In the case of L105H, $\lambda_{max}$ was similar to that of the wild type at both low and high pH, but the p$K_a$ value increased by 1.05 pH unit versus that of the wild type. An increase in the p$K_a$ value was also observed for L105P and L105R, both of which showed a smaller spectral shift upon protonation of Asp97.

**HPLC Analysis of L105 Mutants.** The observed variation in $\lambda_{max}$ and p$K_a$ is presumably the result of the direct interaction of the retinal chromophore and the amino acid residue at position 105, where molecular properties of each residue are strongly influenced, including volume, charge, polarity, and molecular shape. In this study, we discuss the molecular mechanism of such an interaction in detail. It should be noted, however, that the amino acid residue at position 105 may also influence the isomeric ratio of the chromophore. The chromophore-binding pocket of microbial rhodopsins accommodates both all-*trans* and 13-*cis*,15-*syn* retinal in the dark, between which only the former has proton pumping activity in PR.[1] As a consequence, the all-*trans* form is predominant (93.4% at pH 4.0 and 95.1% at pH 9.6)


dx.doi.org/10.1021/bi500842w | *Biochemistry* 2014, 53, 6032−6040

**Table 2. Properties of the Wild-Type and 19 Position 105 Mutant Proteins**

| | | $\lambda_{max}$ measured (nm) | | $\lambda_{max}$ from curve fitting (nm) | | | |
|---|---|---|---|---|---|---|---|
| | volume ($cm^3$/mol) | low pH | high pH | deprotonated | pH 8 | protonated | p$K_a$ |
| wild type | 99.1 | 545 (4.0) | 516 (9.6) | 517.0 | 518.8 | 542.6 | 6.87 |
| L105G | 34.8 | 523 (4.0) | 496 (10.1) | 497.8 | 501.3 | 521.8 | 7.26 |
| L105S | 51.9 | 533 (5.5) | 499 (9.5) | 500.1 | 501.6 | 531.1 | 6.73 |
| L105A | 52.0 | 556 (5.7) | 502 (10.0) | 503.6 | 506.0 | 556.1 | 6.64 |
| L105C | 65.0 | 551 (5.6) | 512 (10.0) | 514.0 | 518.1 | 548.4 | 7.10 |
| L105D | 65.4 | 547 (5.0) | 510 (10.0) | 510.4 | 516.3 | 543.8 | 7.27 |
| L105T | 68.4 | 548 (5.0) | 503 (9.8) | 503.9 | 509.2 | 546.0 | 7.14 |
| L105N | 69.6 | 548 (5.5) | 512 (9.5) | 513.6 | 519.6 | 544.1 | 7.39 |
| L105P | 72.6 | 535 (4.4) | 520 (9.9) | 522.4 | 528.9 | 534.4 | 8.13 |
| L105E | 77.5 | 538 (4.9) | 499 (10.1) | 500.5 | 502.1 | 536.1 | 6.67 |
| L105V | 82.4 | 571 (5.7) | 523 (10.0) | 523.4 | 540.9 | 567.6 | 7.85 |
| L105Q | 85.5 | 536 (4.9) | 493 (10.0) | 494.5 | 499.0 | 535.6 | 7.10 |
| L105H | 90.4 | 544 (5.5) | 512 (10.0) | 513.4 | 526.0 | 540.5 | 7.92 |
| L105M | 96.9 | 552 (5.5) | 524 (10.0) | 524.7 | 534.1 | 550.1 | 7.79 |
| L105I | 99.1 | 555 (5.0) | 517 (9.7) | 518.7 | 528.5 | 552.7 | 7.63 |
| L105K | 100.1 | 560 (5.5) | 529 (10.0) | 532.4 | 538.5 | 556.8 | 7.53 |
| L105F | 112.8 | 564 (5.6) | 527 (10.0) | 531.4 | 539.0 | 559.6 | 7.58 |
| L105Y | 114.7 | 564 (6.0) | 524 (10.7) | 528.1 | 546.0 | 561.5 | 8.07 |
| L105R | 118.9 | 529 (6.6) | 514 (9.9) | 513.8 | 525.3 | 527.8 | 8.69 |
| L105W | 135.5 | 562 (6.0) | 527 (10.4) | 529.4 | 542.6 | 558.8 | 7.91 |

in wild-type PR. Nevertheless, L105X PR may contain an increased level of 13-*cis*,15-*syn* retinal, or even other isomeric states such as 11-*cis* and 9-*cis*, which could be a reason for the observed absorption properties. Therefore, we examined the isomeric composition of the wild type and 19 L105 mutants at low and high pH in the dark using HPLC analysis.

Figure S2 of the Supporting Information shows typical HPLC patterns. In the case of the wild type, the content of the all-*trans* form accounted for 92 and 95% at low and high pH, respectively, indicating that the functionally active form is predominant. Table 1 illustrates similar results for most of the L105 mutants where the contents of the all-*trans* form accounted for >80% at both low and high pH, except for three mutants, L105P, L105Y, and L105W. L105P primarily contains 11-*cis* (11.5% at low pH and 9.5% at high pH) and 9-*cis* (13.3% at low pH and 9.7% at high pH) forms. On the other hand, the content of 13-*cis* was low. The all-*trans* content was lowest for L105Y, which contains 13-*cis* (9.1% at low pH and 11.0% at high pH), 11-*cis* (10.2% at low pH and 10.6% at high pH), and 9-*cis* (9.2% at low pH and 7.9% at high pH) forms. In contrast, L105W contains exclusively 13-*cis* (10.9% at low pH and 17.8% at high pH). Figure S3 of the Supporting Information shows that the content of the all-*trans* form gradually decreased when the volume of the residue at position 105 increased.

These *cis* components may influence the observed absorption properties of L105P, L105Y, and L105W. It is, however, noted that the spectral separation of the all-*trans* and *cis* forms needs additional parameters such as absorption spectra and isomeric ratios at different temperatures, which is complicated. Because the isomeric composition of the all-*trans* chromophore is >70% for all samples, we did not study further the absorption properties of *cis* components in this paper. Next, we describe the analysis of these data by considering characteristics of amino acid residues such as hydropathy and volume.

**Correlation of $\lambda_{max}$ and Counterion p$K_a$ Values.** From the data in Figure 3, the $\lambda_{max}$ values of species with both protonated and deprotonated Asp97 and the counterion p$K_a$ were obtained for 20 amino acid residues at position 105 (Table 2). Figure 4 shows the correlation between $1/\lambda_{max}$ of the species with deprotonated (a) and protonated (b) Asp97 and the p$K_a$ of Asp97, which were obtained from the values in the fitting curve of the Henderson−Hasselbalch equation in Figure 3 (see the values of curve fitting in Table 1). There was a tiny correlation between the $\lambda_{max}$ of the species with deprotonated Asp97 and the p$K_a$ of Asp97 (Figure 4a), but no correlation between the $\lambda_{max}$ of the species with protonated Asp97 and the p$K_a$ of Asp97 (Figure 4b). Such a weak correlation between $\lambda_{max}$ and the counterion p$K_a$ is an unexpected result.

We previously reported linear relationships between the $\lambda_{max}$ of species with deprotonated and protonated Asp97 and the p$K_a$ of Asp97 in the case of A178 mutants of PR.[21] This is reasonable because the interaction between the protonated Schiff base and its counterion is a key element in determining the $\lambda_{max}$ and p$K_a$ of the counterion.[1] In general, as the interaction becomes stronger, the $\lambda_{max}$ is more blue-shifted because of the localization of the positive charge at the Schiff base, and the p$K_a$ of the counterion is lowered because of the preferable ion-pair state. Consequently, a blue-shifted $\lambda_{max}$ is correlated with a low p$K_a$. This was indeed the case for the wild type and 19 mutants of A178 PR, the amino acid residue located at the E−F loop.[21] If so, then why was no linear relationship observed for the L105 mutants PR? This observation suggests a complicated process for determining the $\lambda_{max}$ and p$K_a$ of the counterion. In the previous study, the mutation site was very distant from the Schiff base region, and each mutation did not specifically control the values of $\lambda_{max}$ and the counterion p$K_a$.[21] In contrast, because Leu105 and Asp97 are close to each other, the L105 mutations possibly affect the local environment of Asp97. In particular, the hydrogen bonding interaction between Asp97 and His75 may be differently influenced by the L105 mutations.[14,28,29]

**Dependence of $\lambda_{max}$ and Counterion p$K_a$ Values on Amino Acid Residue Hydrophobicity.** We then correlated $\lambda_{max}$ and p$K_a$ with the properties of each amino acid residue. Because GPR and BPR possess Leu and Gln at position 105, respectively, we first considered that the hydrophobicity of amino acid residue is a key element in color tuning. In fact, it is


dx.doi.org/10.1021/bi500842w | *Biochemistry* 2014, 53, 6032−6040

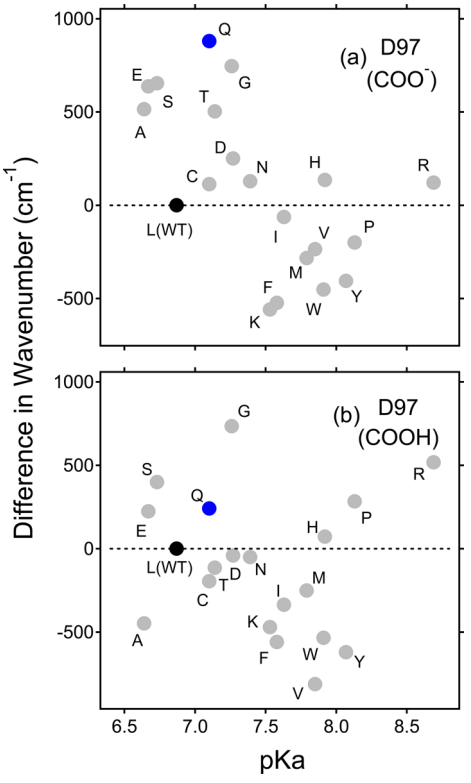


**Figure 4.** Correlation between the absorption light energy of the species with (a) deprotonated or (b) protonated Asp97, and the p$K_a$ value of Asp97 in L105X GPR. The *y*-axis represents the difference in wavenumber from that of the wild type (reciprocal $\lambda_{max}$; $cm^{-1}$), where positive and negative values correspond to the spectral blue- and red-shifts, respectively. The $\lambda_{max}$ values of the (a) deprotonated and (b) protonated forms were obtained from the values at high and low pH, respectively, in the fitting curve of the Henderson−Hasselbalch equation in Figure 3 (see the values of curve fitting in Table 1). The p$K_a$ of Asp97 was similarly obtained from the Henderson−Hasselbalch equation in Figure 3 (see the p$K_a$ values in Table 1).

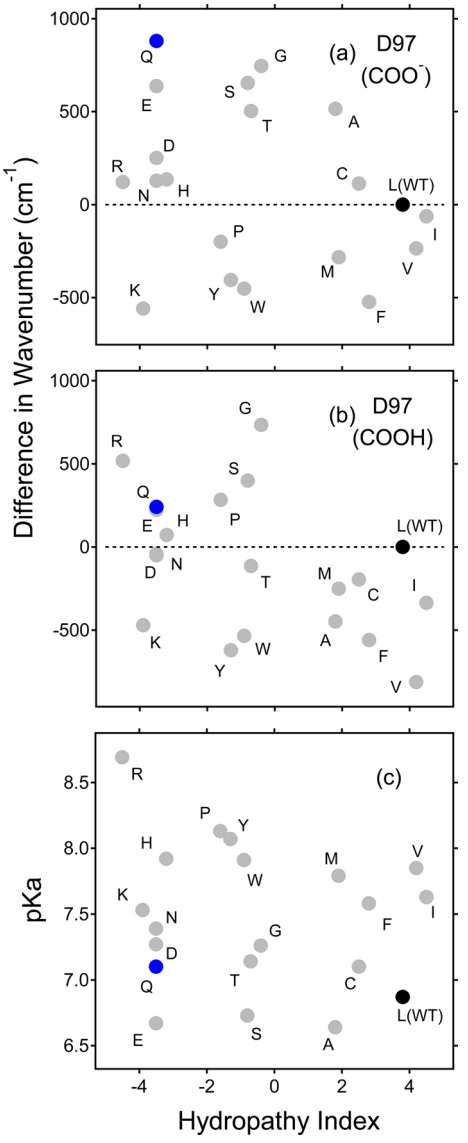


**Figure 5.** Correlation between the absorption light energy of the species with (a) deprotonated Asp97, (b) protonated Asp97, or (c) the p$K_a$ value of Asp97 and the hydropathy index of the amino acid residue at position 105 in L105X GPR. The *y*-axis in panels a and b represents the difference in wavenumber from that of the wild type (reciprocal $\lambda_{max}$; $cm^{-1}$), where positive and negative values correspond to the spectral blue- and red-shifts, respectively. The $\lambda_{max}$ values of the (a) deprotonated and (b) protonated forms were obtained from the value at high and low pH, respectively, in the fitting curve of the Henderson−Hasselbalch equation in Figure 3 (see the values of curve fitting in Table 1). The p$K_a$ of Asp97 (c) was similarly obtained from the Henderson−Hasselbalch equation in Figure 3 (see the p$K_a$ values in Table 1).

known that the cytoplasmic side of the retinal chromophore is highly hydrophobic[1] and that the hydrophobicity or hydrophilicity of amino acid residues must affect the $\lambda_{max}$ and p$K_a$ value of Asp97. Panels a and b of Figure 5 show the correlation between the hydropathy index of the amino acid residue at position 105 and $1/\lambda_{max}$ of the species with deprotonated and protonated Asp97, respectively. Similarly, Figure 5c shows the correlation between the hydropathy index of the residue at position 105 and the p$K_a$ of Asp97. Surprisingly, there was almost no correlation with the hydropathy index. Figure 5a shows that the most blue-shifted amino acid residue is Gln for the deprotonated D97 form, whereas there was no correlation with the hydrophobicity or hydrophilicity of amino acid residues. This is also the case for the protonated D97 form (Figure 5b) and p$K_a$ (Figure 5c). Although GPR and BPR at position 105 naturally selected highly hydrophobic (Leu) and hydrophilic (Gln) amino acid residues, respectively, hydrophobicity or hydrophilicity is not a determinant of the color of PR.

**Dependence of $\lambda_{max}$ and Counterion p$K_a$ Values on Amino Acid Residue Volume.** We next tested the correlation with the volume of amino acid residues. Figure 6 shows the correlation between the volume of the amino acid residue at position 105 and $1/\lambda_{max}$ of the species (a) with deprotonated Asp97, (b) at pH 8, and (c) with protonated Asp97. In contrast to the hydropathy index, the obtained $\lambda_{max}$ values were clearly dependent on the volume of the residue at position 105, where $\lambda_{max}$ was red-shifted, as the volume was larger. This observation is in contrast to a simple idea that a large volume at position 105 moves the chromophore toward the counterion (Asp97), by which a spectral blue-shift is predicted by a stronger chromophore−counterion interaction. Thus, our results suggest that as the volume becomes larger, the chromophore is apparently moved toward the opposite side of the counterion. The slopes of the linear correlation in panels a−c of Figure 6 are −12.3, −12.2, and −7.2 $cm^{-1}$ $cm^{-3}$ mol, respectively, indicating that the dependence on volume is weaker for the protonated


dx.doi.org/10.1021/bi500842w | *Biochemistry* 2014, 53, 6032−6040

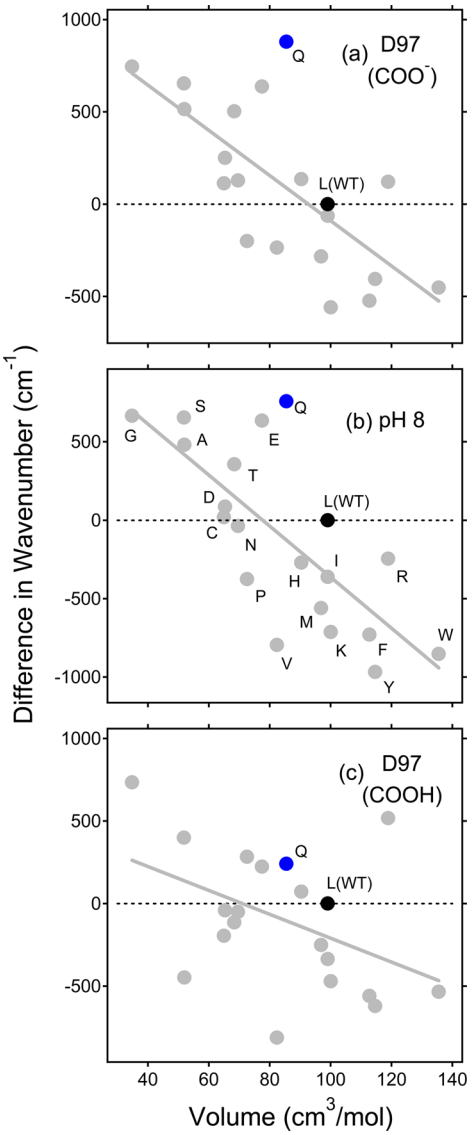


**Figure 6.** Correlation between the absorption light energy of the species (a) with deprotonated Asp97, (b) at pH 8, or (c) with protonated Asp97 and the volume of the amino acid residue at position 105 in L105X GPR. The *y*-axis represents the difference in wavenumber from that of the wild type (reciprocal $\lambda_{max}$; $cm^{-1}$), where positive and negative values correspond to the spectral blue- and red-shifts, respectively. The $\lambda_{max}$ values in panels a−c were obtained from the values at high pH, pH 8, and low pH, respectively, in the fitting curve of the Henderson−Hasselbalch equation in Figure 3 (see the values of curve fitting in Table 1). Gray solid lines represent the results of linear approximation.

Asp97. According to the linear correlation, the introduction of a methyl group (17 $cm^3$/mol) causes a spectral red-shift of 200 $cm^{-1}$ (~5.0 nm) under physiological conditions (pH 8).

Some amino acid residues deviated from a linear correlation, the greatest being L105Q, the residue of BPR. In fact, the size of the amino acid residue was similar between Leu and Gln, but L105Q exhibited the most blue-shifted $\lambda_{max}$ for the deprotonated D97 form (Figure 6a) and for the native environment [pH 8 (Figure 6b)]. This implies a specific interaction of Gln105 with the retinal chromophore during evolution. It is possible that the C═O group of Gln105 yields localization of the positive charge at the Schiff base region by interacting with the C15-H group, as suggested by a theoretical study.[30]

Figure 7 shows that there is the same correlation between residue volume at position 105 and the p$K_a$ of Asp97 as for $\lambda_{max}$.

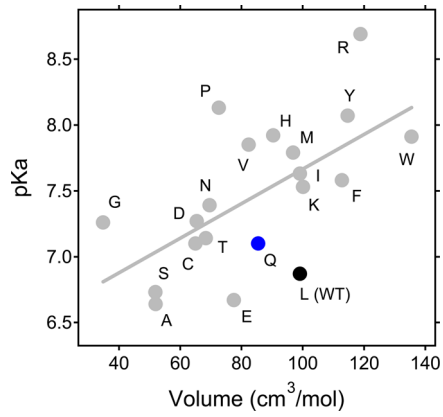


**Figure 7.** Correlation between the p$K_a$ of Asp97 and the volume of the amino acid residue at position 105 in L105X GPR. The p$K_a$ of Asp97 was obtained from the Henderson−Hasselbalch equation in Figure 3 (see the p$K_a$ values in Table 1). Gray solid line represents the result of linear approximation.

The p$K_a$ of Asp97 increased when the volume was larger. L105 and L105Q, corresponding to GPR and BPR, respectively, kept the p$K_a$ of the counterion low compared to those with other amino acid residues that have a similar side chain volume, for example, Val, His, Met, Ile, and Lys. This low p$K_a$ is suitable for proton pumping activity because only the deprotonated form of the counterion is the functional state of proton pumping activity.

## DISCUSSION

To understand the role of Leu105 in color tuning, structural information is a prerequisite. Many efforts in solid-state[31−34] and solution[35] NMR and X-ray crystallography[14,15,36] with GPR and similar proteins have provided its structure, in which Leu105 is in contact with the retinal chromophore. This is supported by resonance Raman spectroscopy of GPR reconstituted into lipid bilayers.[37] Our HPLC analysis shows that the all-*trans* chromophore is responsible for color tuning in L105X proteins, where volume is more important as a determinant than hydrophobicity. We discuss the mechanism below.

**Color Tuning Mechanism of the L/Q Switch.** In color tuning, three factors are normally considered: (i) chromophore distortion, (ii) electrostatic interaction between the protonated Schiff base and the counterion, and (iii) polarity around the $\beta$-ionone ring and the polyene chain.[1] In general, we expect a spectral blue-shift when the chromophore is distorted (mechanism i), because chromophore distortion breaks $\pi$-electron conjugation along the polyene chain. A blue-shift is also expected when the Schiff base−counterion interaction is strong (mechanism ii), because a positive charge is localized near the Schiff base. These two factors have a stronger influence on color tuning than the third, but we expect a spectral blue-shift when the environment around the $\beta$-ionone ring and polyene chain is less polar (mechanism iii), because a polar environment yields delocalization of the positive charge out of the Schiff base. Leu105 is located at a critical position in the structure of microbial rhodopsin. Leu105 and Asp97 sandwich the retinal chromophore from the cytoplasmic and extracellular sides, respectively, where Leu105 constitutes the retinal binding pocket


dx.doi.org/10.1021/bi500842w | *Biochemistry* 2014, 53, 6032−6040

near the polyene chain, but also close to the Schiff base (Figure 1).

A positive correlation with volume, but not with hydropathy, is explained in terms of three factors in color tuning. First, chromophore distortion (mechanism i) is unlikely, though this study does not provide any structural information. In fact, if large amino acid residues cause chromophore distortion by a volume effect, we expect a spectral blue-shift for large amino acid residues. Nevertheless, we observed a spectral red-shift for large residues (Figure 6). A small effect on isomeric composition (Figures S2 and S3 of the Supporting Information), except for L206P, -Y, and -W, supports this interpretation. The same discussion is possible for the Schiff base−counterion interaction (mechanism ii). If introduction of large residues into position 105 shortens the distance between the Schiff base and counterion, we expect a spectral blue-shift for large residues. Nevertheless, we observed a spectral red-shift for large residues (Figure 6). A volume effect seems to work counter to what we know about the mechanism, which was surprising.

We originally expected the contribution of mechanism iii because Leu and Gln differ in hydropathy, but not volume. Mechanism iii implies that introduction of a polar group into the ring/polyene or Schiff base region causes delocalization or localization of a positive charge, leading to a spectral red- or blue-shift. Position 105 in GPR is located along the polyene chain, but also close to the Schiff base, and mechanism iii may act on color tuning in a complicated way. No correlation between color tuning and hydropathy (Figure 5) supports this notion.

Then, why is color tuning correlated with volume? It is obvious that general mechanisms (i−iii) are not sufficient to explain our observation. Therefore, we infer the presence of two different mechanisms for large and small volumes. It should be noted that the water-containing hydrogen-bonding network is optimized in the Schiff base region.[38] It is thereby possible that introduction of large amino acid residues into position 105 disrupts the hydrogen-bonding network in the Schiff base region, leading to a weakened interaction between the Schiff base and counterion (Asp97). This hypothesis is consistent with the positive correlation between the volume and p$K_a$ of the counterion (Figure 7). For small amino acid residues, we suggest that the hydrogen-bonding network is probably retained in the Schiff base region. To compensate for a samller volume, water molecules may penetrate into the cavity, which contributes to the stabilization of the protein structure. It is likely that water molecules tend to be positioned near the Schiff base rather than the polyene chain, which contributes to localization of a positive charge at the Schiff base and leads to a spectral blue-shift. Our interpretation is based on the stable hydrogen-bonding network in the Schiff base, where a negatively charged counterion (Asp97) is more important than a neutral counterion. This is fully consistent with the results in Figure 6, where dependence on volume is clearer for the deprotonated D97 (Figure 6a) than for the protonated D97 (Figure 6c).

## CONCLUSION

The L/Q switch at position 105 controls the color of PR, where GPR and BPR possess Leu and Gln, hydrophobic and hydrophilic amino acid residues, respectively. Nevertheless, this comprehensive mutation study of L105X GPR revealed no correlation between absorbing wavelengths and the hydropathy index of residues. In contrast, absorbing wavelengths and the p$K_a$ value of the Schiff base counterion (Asp97) were correlated with the volume of residues, even though Gln and Leu have similar volumes. We infer that the local and specific interaction in the Schiff base moiety determines the $\lambda_{max}$ and p$K_a$ of Asp97, which is more influenced by the volume of the residue at position 105 than by its hydrophobicity. For large amino acid residues, the hydrogen-bonding network in the Schiff base moiety is significantly perturbed, and a weakened interaction between the Schiff base and Asp97 leads to a spectral red-shift. This view is also consistent with the increased p$K_a$ of Asp97 for large residues (Figure 7). For small residues, while the hydrogen-bonding network is retained in the Schiff base moiety, water molecules may be introduced into the Schiff base region. Additional protein-bound water molecules in the Schiff base region possibly localize the positive charge at the Schiff base, leading to the spectral red-shift. Other interpretations may be possible, and our hypothesis needs to be examined by structural analysis. It is also noted that these data, such as the $\lambda_{max}$ and p$K_a$ of Asp97 in L105X GPR, should be reproduced *in silico*, which is challenging in the field of theoretical calculation. Discussion related to evolutionary processes in GPR and BPR is also intriguing, so much so that we are now able to discuss how the color tuning mechanism has been optimized for microbial rhodopsins in marine bacteria.

## ASSOCIATED CONTENT

### Supporting Information

Typical pH-dependent absorption spectra (Figure S1), typical HPLC pattern (Figure S2), and volume dependence of the isomeric ratio of the all-*trans* form for the wild type and 19 position 105 mutant proteins (Figure S3). This material is available free of charge via the Internet at http://pubs.acs.org.

## AUTHOR INFORMATION

### Corresponding Author

*Department of Frontier Materials, Nagoya Institute of Technology, Showa-ku, Nagoya 466-8555, Japan. Phone and fax: 81-52-735-5207. E-mail: kandori@nitech.ac.jp.

### Funding

This work was supported by a grant from the Japanese Ministry of Education, Culture, Sports, Science and Technology to H.K. (25104009).

### Notes

The authors declare no competing financial interest.

## ABBREVIATIONS

PR, proteorhodopsin; BPR, blue-absorbing proteorhodopsin; GPR, green-absorbing proteorhodopsin; BR, bacteriorhodopsin; ESR, *E. sibiricum* rhodopsin; DDM, dodecyl maltoside.

## REFERENCES

(1) Ernst, O. P., Lodowski, D. T., Elstner, M., Hegemann, P., Brown, L. S., and Kandori, H. (2014) Microbial and animal rhodopsins: Structure, functions, and molecular mechanisms. *Chem. Rev. 114*, 126−163.

(2) Kochendoerfer, G. G., Lin, S. W., Sakmar, T. P., and Mathies, R. A. (1999) How color visual pigments are tuned. *Trends Biochem. Sci. 24*, 300−305.

(3) Kakitani, T., Beppu, Y., and Yamada, A. (1999) Color tuning mechanism of human red and green visual pigments. *Photochem. Photobiol. 70*, 686−693.

(4) Shimono, K., Hayashi, T., Ikeura, Y., Sudo, Y., Iwamoto, M., and Kamo, N. (2003) Importance of the broad regional interaction for spectral tuning in *Natrobacterium pharaonis* phoborhodopsin (sensory rhodopsin II). *J. Biol. Chem. 278*, 23882−23889.

(5) Hoffmann, M., Wanko, M., Stodel, P., Konig, P. H., Frauenheim, T., Schulten, K., Thiel, W., Tajkhorshid, E., and Elstner, M. (2006) Color

tuning in rhodopsins: The mechanism for the spectral shift between bacteriorhodopsin and sensory rhodopsin II. *J. Am. Chem. Soc. 128*, 10808−10818.
(6) Coto, P. B., Strambi, A., Ferre, N., and Olivucci, M. (2006) The color of rhodopsins at the ab initio multiconfigurational perturbation theory resolution. *Proc. Natl. Acad. Sci. U.S.A. 103*, 17154−17159.
(7) Sekharan, S., Katayama, K., Kandori, H., and Morokuma, K. (2012) Color vision: "OH-site" rule for seeing red and green. *J. Am. Chem. Soc. 134*, 10706−10712.
(8) Sudo, Y., Okazaki, A., Ono, H., Yagasaki, J., Sugo, S., Kamiya, M., Reissig, L., Inoue, K., Ihara, K., Kandori, H., Takagi, S., and Hayashi, S. (2013) A blue-shifted light-driven proton pump for neural silencing. *J. Biol. Chem. 288*, 20624−20632.
(9) Beja, O., Spudich, E. N., Spudich, J. L., Leclerc, M., and DeLong, E. F. (2001) Proteorhodopsin phototrophy in the ocean. *Nature 411*, 786−789.
(10) Bamann, C., Bamberg, E., Wachtveitl, J., and Glaubitz, C. (2014) Proteorhodopsin. *Biochim. Biophys. Acta 1837*, 614−625.
(11) Beja, O., Aravind, L., Koonin, E. V., Suzuki, M. T., Hadd, A., Nguyen, L. P., Jovanovich, S. B., Gates, C. M., Feldman, R. A., Spudich, J. L., Spudich, E. N., and DeLong, E. F. (2000) Bacterial rhodopsin: Evidence for a new type of phototrophy in the sea. *Science 289*, 1902−1906.
(12) Wang, W. W., Sineshchekov, O. A., Spudich, E. N., and Spudich, J. L. (2003) Spectroscopic and photochemical characterization of a deep ocean proteorhodopsin. *J. Biol. Chem. 278*, 33985−33991.
(13) Man, D., Wang, W., Sabehi, G., Aravind, L., Post, A. F., Massana, R., Spudich, E. N., Spudich, J. L., and Beja, O. (2003) Diversification and spectral tuning in marine proteorhodopsins. *EMBO J. 22*, 1725−1731.
(14) Ran, T., Ozorowski, G., Gao, Y., Sineshchekov, O. A., Wang, W., Spudich, J. L., and Luecke, H. (2013) Cross-protomer interaction with the photoactive site in oligomeric proteorhodopsin complexes. *Acta Crystallogr. D69*, 1965−1980.
(15) Gushchin, I., Chervakov, P., Kuzmichev, P., Popov, A., Round, E., Borshchevskiy, V., Dolgikh, D., Kirpichnikov, M., Petrovskaya, L., Chupin, V., Arseniev, A., and Gordeliy, V. (2013) Structural insights into the proton pumping by unusual proteorhodopsin from nonmarine bacteria. *Proc. Natl. Acad. Sci. U.S.A. 110*, 12631−12636.
(16) Subramaniam, S., Greenhalgh, D. A., Rath, P., Rothschild, K. J., and Khorana, H. G. (1991) Replacement of leucine-93 by alanine or threonine slows down the decay of the N and O intermediates in the photocycle of bacteriorhodopsin: Implications for proton uptake and 13-*cis*-retinal → all-*trans*-retinal reisomerization. *Proc. Natl. Acad. Sci. U.S.A. 88*, 6873−6877.
(17) Maiti, T. K., Yamada, K., Inoue, K., and Kandori, H. (2012) L105K mutant of proteorhodopsin. *Biochemistry 51*, 3198−3204.
(18) Yoshitsugu, M., Shibata, M., Ikeda, D., Furutani, Y., and Kandori, H. (2008) Color change of proteorhodopsin by a single amino acid replacement at a distant cytoplasmic loop. *Angew. Chem., Int. Ed. 47*, 3923−3926.
(19) Krebs, R. A., Alexiev, U., Partha, R., DeVita, A. M., and Braiman, M. S. (2002) Detection of fast light-activated $H^+$ release and M intermediate formation from proteorhodopsin. *BMC Physiol. 2*, 5.
(20) Yoshitsugu, M., Yamada, J., and Kandori, H. (2009) Color-changing mutation in the E-F loop of proteorhodopsin. *Biochemistry 48*, 4324−4330.
(21) Yamada, K., Kawanabe, A., and Kandori, H. (2010) Importance of alanine at position 178 in proteorhodopsin for absorption of prevalent ambient light in the marine environment. *Biochemistry 49*, 2416−2423.
(22) Kawanabe, A., Furutani, Y., Jung, K. H., and Kandori, H. (2006) FTIR study of the photoisomerization processes in the 13-*cis* and all-*trans* forms of *Anabena* sensory rhodopsin at 77 K. *Biochemistry 45*, 4362−4370.
(23) Dioumaev, A. K., Brown, L. S., Shih, J., Spudich, E. N., Spudich, J. L., and Lanyi, J. K. (2002) Proton transfers in the photochemical reaction cycle of proteorhodopsin. *Biochemistry 41*, 5348−5358.
(24) Friedrich, T., Geibel, S., Kalmbach, R., Chizhov, I., Ataka, K., Heberle, J., Engelhard, M., and Bamberg, E. (2002) Proteorhodopsin is a light-driven proton pump with variable vectoriality. *J. Mol. Biol. 321*, 821−838.
(25) Dér, A., Száraz, S., Tóth-Baconádi, R., Tokaji, Z., Keszthelyi, L., and Stoeckenius, W. (1991) Alternative translocation of protons and halide ions by bacteriorhodopsin. *Proc. Natl. Acad. Sci. U.S.A. 88*, 4751−4755.
(26) Chizov, I., Schmies, G., Seidel, R., Sydor, J. R., Lüttenberg, B., and Engelhard, M. (1998) The photophobic receptor from *Natronobacterium pharaonis*: Temperature and pH dependencies of the photocycle of sensory rhodopsin II. *Biophys. J. 75*, 999−1009.
(27) Shimono, K., Kitami, M., Iwamoto, M., and Kamo, N. (2000) Involvement of two groups in reversal of the bathochromic shift of *pharaonis* phoborhodopsin by chloride at low pH. *Biophys. Chem. 87*, 225−230.
(28) Bergo, V. B., Sineshchekov, O. A., Kralj, J. M., Partha, R., Spudich, E. N., Rothschild, K. J., and Spudich, J. L. (2009) His-75 in proteorhodopsin, a novel component in light-driven proton translocation by primary pumps. *J. Biol. Chem. 284*, 2836−2843.
(29) Hempelmann, F., Hölper, S., Verhoefen, M. K., Woerner, A. C., Köhler, T., Fiedler, S. A., Pfleger, N., Wachtveitl, J., and Glaubitz, C. (2011) His75-Asp97 cluster in green proteorhodopsin. *J. Am. Chem. Soc. 133*, 4645−4654.
(30) Hillebrecht, J. R., Galan, J., Rangarajan, R., Ramos, L., McCleary, K., Ward, D. E., Stuart, J. A., and Brige, R. R. (2006) Structure, function, and wavelength selection in blue-absorbing proteorhodopsin. *Biochemistry 45*, 1579−1590.
(31) Shastri, S., Vonck, J., Pfleger, N., Haase, W., Kuehlbrandt, W., and Glaubitz, C. (2007) Proteorhodopsin: Characterization of 2D crystals by electron microscopy and solid state NMR. *Biochim. Biophys. Acta 1768*, 3012−3019.
(32) Shi, L., Ahmed, M. A., Zhang, W., Whited, G., Brown, L. S., and Ladizhansky, V. (2009) Three-dimensional solid-state NMR study of a seven-helical integral membrane proton pump: Structural insights. *J. Mol. Biol. 386*, 1078−1093.
(33) Pfleger, N., Wörner, A. C., Yang, J., Shastri, S., Hellmich, U. A., Aslimovska, L., Maier, M. S., and Glaubitz, C. (2009) Solid-state NMR and functional studies on proteorhodopsin. *Biochim. Biophys. Acta 1787*, 697−705.
(34) Ward, M. E., Shi, L., Lake, E., Krishnamurthy, S., Hutchins, H., Brown, L. S., and Ladizhansky, V. (2011) Proton-detected solid-state NMR reveals intramembrane polar networks in a seven-helical transmembrane protein proteorhodopsin. *J. Am. Chem. Soc. 133*, 17434−17443.
(35) Reckel, S., Gottstein, D., Stehle, J., Löhr, F., Verhoefen, M. K., Takeda, M., Silvers, R., Kainosho, M., Glaubitz, C., Wachtveitl, J., Bernhard, F., Schwalbe, H., Güntert, P., and Dötsch, V. (2011) Solution NMR structure of proteorhodopsin. *Angew. Chem., Int. Ed. 50*, 11942−11946.
(36) Luecke, H., Schobert, B., Stagno, J., Imasheva, E. S., Wang, J. M., Balashov, S. P., and Lanyi, J. K. (2008) Crystallographic structure of xanthorhodopsin, the light-driven proton pump with a dual chromophore. *Proc. Natl. Acad. Sci. U.S.A. 105*, 16561−16565.
(37) Kralj, J. M., Spudich, E. N., Spudich, J. L., and Rothschild, K. J. (2008) Raman spectroscopy reveals direct chromophore interactions in the Leu/Gln105 spectral tuning switch of proteorhodopsins. *J. Phys. Chem. B 112*, 11770−11776.
(38) Ikeda, D., Furutani, Y., and Kandori, H. (2007) FTIR study of the retinal Schiff base and internal water molecules of proteorhodopsin. *Biochemistry 46*, 5365−5373.